EFFECT OF Fe-Au MODIFICATION ON THE ELECTROCATALYTIC ACTIVITY OF Ni/GDC FUEL ELECTRODE FOR THE INTERNAL CO_2 REFORMING OF CH_4 IN SOFCs

E. Ioannidou[1,*], S.G. Neophytides[1], D.K. Niakolas[1,2]

[1]Foundation for Research and Technology, Institute of Chemical Engineering Sciences (FORTH/ICE-HT), Patras, GR-26504, Greece

[2]Department of Chemistry, University of Ioannina, GR-45110, Greece

(*eioannidou@iceht.forth.gr)

ABSTRACT

This work presents electrocatalytic measurements on Ni/GDC, 1Au-Ni/GDC, 3Au-Ni/GDC, 0.5Fe-1Au-Ni/GDC and 0.5Fe-3Au-Ni/GDC electrocatalysts, in the form of full cells for the internal DRM process, at 900 °C, under a mixture of CH_4/CO_2=1. The electrochemical characterization included i-V, i-P and Electrochemical Impedance Spectroscopy (EIS) measurements, as well as Gas Chromatography (GC) analysis, in order to clarify the effect of the synergistic interaction between Fe-Au-Ni and the effect of polarization on the electrocatalytic performance and on the production/consumption rates.

The experimental data showed that the cells with the ternary 0.5Fe-1Au-Ni/GDC and 0.5Fe-3Au-Ni/GDC performed with the highest power output, whereas they exhibited the lowest R_s and R_p values, compared to the cells with the binary 1Au-Ni/GDC and 3Au-Ni/GDC, implying the synergy of Fe-Au-Ni, regardless the content of Au. Furthermore, the increase of polarization resulted in the deterioration of R_s for the cell with Ni/GDC and this trend can be attributed to the possible gradual re-oxidation and/or agglomeration of Ni, due to the high partial pressures of steam and CO_2 in the reaction mixture during the SOFC operation. On the other hand, the R_s for the cells with the modified electrodes was the least affected by increasing the polarization, which can be correlated with the Fe-Au or Au modification.

KEYWORDS: single SOFCs, Fe-Au-Ni/GDC fuel electrodes, electrocatalytic performance, internal CO_2 reforming of CH_4, degradation

INTRODUCTION

Solid Oxide Fuel Cells (SOFCs) could have a key role as energy producing devices by using renewable sources such as biogas (55-65% CH_4 and 35-45% CO_2), which is obtained by landfills or anaerobic digesters [1].

Biogas can be directly fueled in the SOFCs without the need of an external reformer (Direct Internal Reforming, DIR) which is one of the competitive advantages for the commercialization of these systems [2]. In the DIR process, the generated heat through the electrochemical reactions of fuel is used for the endothermic reforming reactions, which decreases the cooling demand of SOFCs and improves the overall efficiency [3]. Despite the significant progress in developing commercial SOFC systems, the main issue that hinders the widespread use of this technology is the performance degradation of the cells due to high thermal stresses and risk of carbon deposition [3,4].

When biogas is directly fed to the SOFC fuel electrode at temperatures 750-900 °C, various catalytic and electrocatalytic reactions may take place simultaneously on the fuel electrode (Eq. 1-7) [5,6].

$CH_4 + CO_2 \leftrightarrow 2CO + 2H_2$ ΔH^o_{298}= 247 kJ mol^{-1} (1)

$CO_2 + H_2 \leftrightarrow CO + H_2O$ ΔH^o_{298}= 41 kJ mol^{-1} (2)

$CH_4 \leftrightarrow C + 2H_2$ ΔH^o_{298}= 75 kJ mol^{-1} (3)

$H_2 + O^{2-} \leftrightarrow H_2O + 2e^-$ ΔH^o_{298}= −242 kJ mol^{-1} (4)

$CO + O^{2-} \leftrightarrow CO_2 + 2e^-$ ΔH^o_{298}= −283 kJ mol^{-1} (5)

$CH_4 + O^{2-} \leftrightarrow CO + 2H_2 + 2e^-$ ΔH^o_{298}= −37 kJ mol^{-1} (6)

$C(s) + O^{2-} \leftrightarrow CO + 2e^-$ ΔH^o_{298}= −111 kJ mol^{-1} (7)

The main reaction that occurs is Dry Reforming of Methane (DRM) to form syngas (Eq. 1), which is a strongly endothermic process, thermodynamically favored at high temperatures (> 650 ºC) [5]. Together with the DRM reaction, also side reactions can occur such as the Reverse Water Gas Shift (RWGS) (> 825 ºC) (Eq. 2), that lowers the H_2/CO ratio and consumes the valuable H_2, and methane decomposition (> 600 ºC) (Eq. 3), that leads to carbon formation [7]. Electrical energy is then produced through the subsequent exothermic electrochemical oxidation of H_2 and CO, as well as of the supplied CH_4 on the fuel electrode (Eq. 4-6) [6,8]. In these reactions O^{2-} ions came from the oxygen electrode, where O_2 reduction takes place, and diffused to the triple-phase boundary zone where they react with the fuel.

The combination between endothermic and exothermic electrocatalytic reactions results in thermal stresses that eventually lead to the destruction of the fuel electrode structure [9]. Another problem is the presence of carbon deposits on the fuel electrode surface which blocks the catalytic active sites, hinders the mass transfer, increases the electrical conductivity and decreases the ionic conductivity and thus leads to the progressive deterioration of the cell performance [2,4,6,7]. Fortunately, under closed circuit conditions in SOFCs, O^{2-} ions can oxidize the absorbed forms of carbidic species, according to Eq. 7 [2,4,6,10]. However, in this case the removal of the absorbed carbon is restricted to the triple-phase boundary zone [6,10].

Nickel/Gadolinia Doped Ceria (Ni/GDC) is widely used as an electrocatalyst in SOFCs because of its activity and inexpensiveness. However, several stability issues arise under hydrocarbon fuel feed because of carbon deposition, re-oxidation and coarsening of Ni particles [11]. The carbon tolerance and anti-sintering tendency of Ni can be enhanced through modification with small amounts (0.5–3 wt.%) of noble (i.e. Au) or non-noble (i.e. Cu, Co, Fe, Sn, Mo and W) metals, which is a subject of many experimental and theoretical studies for the DRM process and it can be also applied in SOFCs under internal DRM process [5,6,8,12]. Recently, Fe-Au-Mo modified Ni/GDC electrocatalysts were studied from our group towards their performance for the DRM, RWGS and CH_4 decomposition reactions [13]. 3Au-Ni/GDC and 0.5Fe-3Au-Ni/GDC were less active catalytically compared to Ni/GDC, but at the same time they proved effective to suppress the non-desired RWGS reaction and they exhibited high tolerance to carbon formation due to their lower activity for the CH_4 decomposition. Therefore, for the purpose of the presented study, there was a selection among these samples for the electro-catalytic measurements and comparison with the SoA Ni/GDC in the form of full cells for the internal DRM process. Additionally, the decrease of the Au content, from 3 to 1 wt.%, was investigated in order to clarify if 1 wt.% Au could be beneficial for internal CO_2 reforming of CH_4 in SOFC operation, except for the price advantage. In this respect, the synergistic interaction between Fe-Au-Ni was directly correlated with the electrochemical activity of the modified Ni/GDC, highlighting superior performance and stability of the new examined 0.5Fe-1Au-Ni/GDC fuel electrode.

METHODOLOGY

Preparation of powders and cells: X wt.% Au-NiO/GDC and 0.5 wt.% Fe-X wt.% Au-NiO/GDC (where X = 1 or 3 wt.%) were prepared via Deposition (Co-)precipitation method by using the commercial NiO/GDC (65 wt.% NiO-35 wt.% GDC, Marion Technologies) powder as the support and the metal precursors $HAuCl_4$ and $Fe(NO_3)_3x9H_2O$ (Sigma-Aldrich). Full details about synthesis can be found elsewhere [13]. In the following, the electrocatalysts will be reported as 1Au-Ni/GDC, 3Au-Ni/GDC, 0.5Fe-1Au-Ni/GDC and 0.5Fe-3Au-Ni/GDC. The electrolyte-supported single fuel cells consisted of a

circular shaped disk ZrO_2 (8%mol Y_2O_3) or 8YSZ electrolyte (Kerafol) with 25 mm diameter and 300 μm thickness. The fuel and oxygen electrodes were deposited on 8YSZ disks via screen-printing. The slurry was composed of a proper amount of powder, terpineol (Sigma-Aldrich) as solvent and polyvinyl butyral (PVB, Sigma-Aldrich) as binder. The electrodes were calcined at 1150 °C/2 h with a heating/cooling ramp rate of 2 °C/min. The resulting loading of the fuel electrode layer was kept low for NiO/GDC (6 mg cm^{-2}), in order to avoid technical problems due to carbon deposition, and was fixed at 10-12 mg cm^{-2} for the modified NiO/GDC electrodes. The oxygen electrode was $La_{0.6}Sr_{0.4}Co_{0.8}Fe_{0.2}O_{3-\delta}$ (LSCoF, SolydEra) with a loading of 10 mg cm^{-2}. In the oxygen side, an adhesion layer of GDC10 (10 mg cm^{-2}) was applied and pre-calcined at 1300 °C/2 h (2 °C/min), in order to overcome the thermal and chemical mismatch between LSCoF-8YSZ.

Electrocatalytic measurements: Each electrocatalyst constituted the only functional layer of the fuel electrode. Ni and Pt mesh gauges (Alfa-Aesar) were used as current collectors on the fuel and oxygen side, respectively. The fuel compartment was fed with a mixture of CH_4/CO_2=1, without dilution in a carrier gas, whereas the oxygen compartment was exposed to 100 vol.% O_2. The lines and valves of the setup were kept above 100 °C to prevent condensation of the produced steam. The flow rates were adjusted at 50 cm^3 min^{-1} in the fuel compartment and 100 cm^3 min^{-1} in the oxygen compartment. In all cases, before the internal DRM measurements, the fuel side of the cells was kept for 24 h in 100 vol.% H_2 (150 cm^3 min^{-1}) in order to be activated. Polarization i-V curves were recorded, by using a potentiostat/galvanonstat, (Autolab PGSTAT30), between the open circuit potential and 0 V, at a scan rate of 5 mV s^{-1} and a step potential of 20 mV. Subsequent Electrochemical Impedance spectra (EIS) were measured in galvanostatic mode at various current densities, with an amplitude that was each time 10% of the applied current, in the frequency range from 100 kHz to 20 mHz. Reactants and products were determined, under both open circuit potential (OCP) and polarization (under various current densities) conditions by using an on-line gas chromatograph (GC, Varian CP-3800) with a thermal conductivity detector.

RESULTS AND DISCUSSION

Fig. 1 shows the characteristic i-V and i-P curves of the SOFCs comprising Ni/GDC, 1Au-Ni/GDC, 3Au-Ni/GDC, 0.5Fe-1Au-Ni/GDC and 0.5Fe-3Au-Ni/GDC as fuel electrodes, under a mixture of CH_4/CO_2=1, without dilution in a carrier gas, at 900 °C.

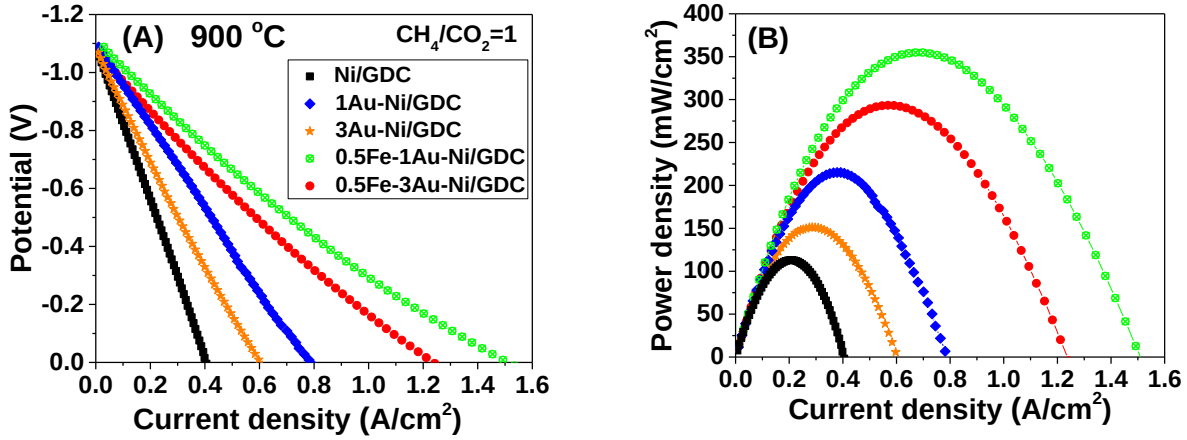

Figure 1. *(**A**) Polarization (i-V) and (**B**) power density curves, at 900 °C, for SOFCs comprising Ni/GDC, 1Au-Ni/GDC, 3Au-Ni/GDC, 0.5Fe-1Au-Ni/GDC and 0.5Fe-3Au-Ni/GDC, as fuel electrodes.*

Specifically, the cells with 0.5Fe-1Au-Ni/GDC and 0.5Fe-3Au-Ni/GDC exhibited the highest activity, since they provided in a wider range of current density values at the same applied potential range and exhibited the highest output power, compared to the other cells. In addition, the cells

with 1Au-Ni/GDC and 3Au-Ni/GDC performed better than that with Ni/GDC, but worse than that with Fe-Au-Ni/GDC samples. The cell with Ni/GDC exhibited the worst electrocatalytic performance for the IDRM process, despite its higher DRM catalytic activity [13].

In order to further elucidate the synergy of Fe-Au-Ni transition metals on the electrochemical processes of the cells, EIS analysis was performed. More specifically, the effect of modification on the ohmic and polarization characteristics of the cells is presented on the Nyquist ($-Z_{im}$ vs. Z_{re}) plots under various applied polarizations (**Fig. 2**). In these plots, the ohmic resistance, R_s, as well as the polarization resistance, R_p, are determined by the intersections of the Z_{re} axis with each Nyquist plot at high and low frequencies respectively. Additionally, the impedance spectra for the modified cells were recorded in a wider range of applied current density values, compared to the cell with Ni/GDC, because the modified cells performed better. The highest applied current density value for each cell corresponded to a potential value close to ~0 V and it should be mentioned that the duration of each measurement at the latter potential, was short ~10 min, in order to avoid the detrimental re-oxidation of the electrodes.

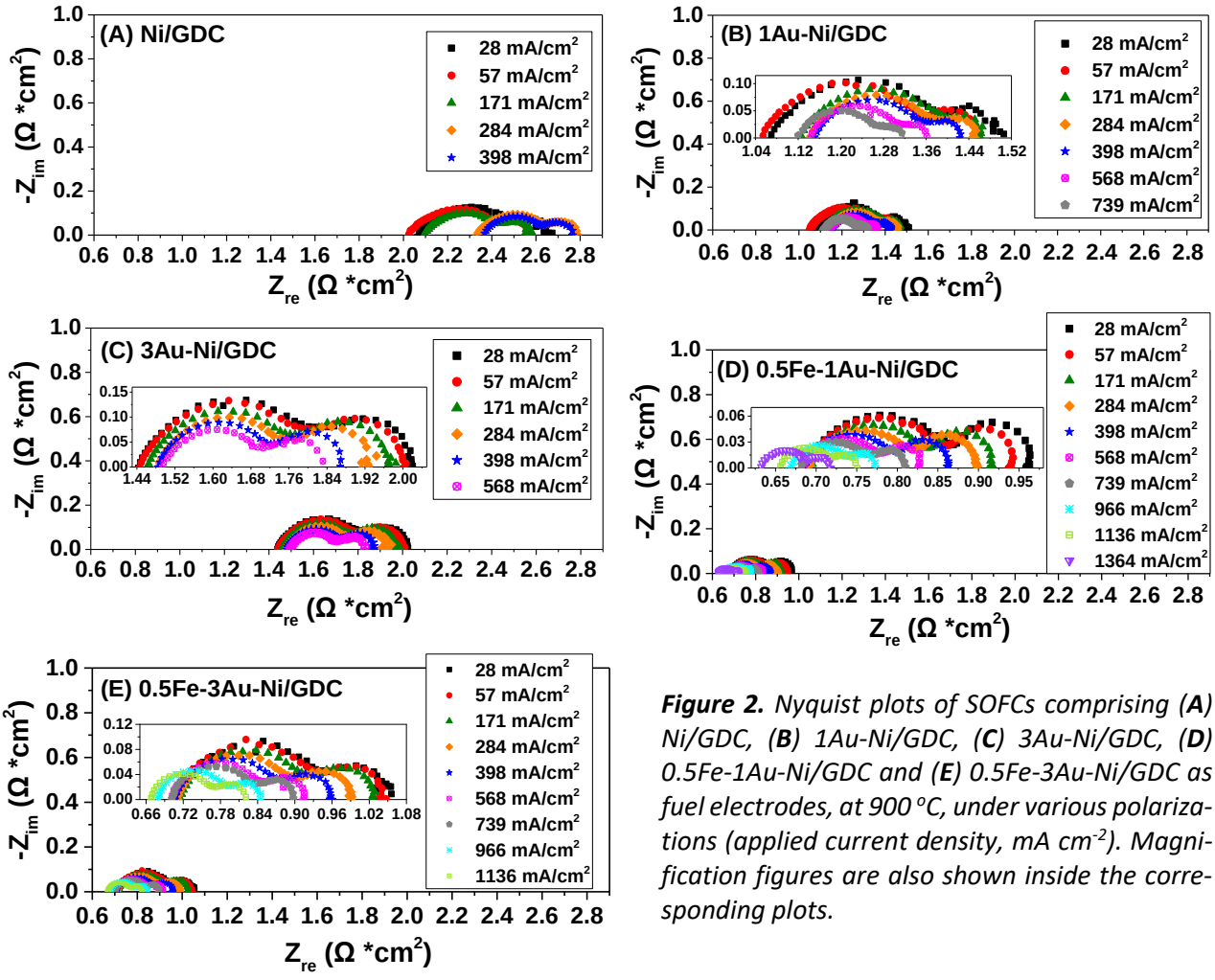

Figure 2. *Nyquist plots of SOFCs comprising (**A**) Ni/GDC, (**B**) 1Au-Ni/GDC, (**C**) 3Au-Ni/GDC, (**D**) 0.5Fe-1Au-Ni/GDC and (**E**) 0.5Fe-3Au-Ni/GDC as fuel electrodes, at 900 °C, under various polarizations (applied current density, mA cm^{-2}). Magnification figures are also shown inside the corresponding plots.*

The impedance characteristics of the system are dominated by two impedance depressed arcs in the Nyquist plots, with the size of the higher frequencies (HF) arc being larger than that of the lower frequencies (LF) arc. In addition, for each cell, as expected and regardless the modification, both LF and HF arcs decrease by increasing the polarization.

Regarding the effect of modification, it is observed that the size of both LF and HF arcs in the Nyquist plots of the cells with 0.5Fe-1Au-Ni/GDC and 0.5Fe-3Au-Ni/GDC, under the same polarization is the smallest compared to the other cells. In addition, the cell with 0.5Fe-3Au-Ni/GDC showed

smaller LF and HF arcs than that with 3Au-Ni/GDC and 1Au-Ni/GDC, but slightly larger than that with 0.5Fe-1Au-Ni/GDC. The above interpretations are followed by variations on R_s and R_p values. Under the same polarization, the cells with 0.5Fe-1Au-Ni/GDC and 0.5Fe-3Au-Ni/GDC exhibited the lowest R_s and R_p values compared to the others. In addition, the cells with 1Au-Ni/GDC and 3Au-Ni/GDC showed higher R_s and R_p values compared to that with Au-Fe-Ni/GDC, which at the same time, were lower than that of the cell with Ni/GDC. The fact that the modified cells exhibited lower R_s and R_p values, compared to the unmodified, can be primarily ascribed to the higher electron conductivity and improved structural properties of the electrochemical interface between the metal phases of Ni-Fe-Au or Ni-Au with GDC and the electrolyte [13,14]. Especially the enhanced electrochemical characteristics of the cells with Fe-Au modified electrodes indicate a synergy of Fe-Au-Ni via the formed solid solution upon H_2-reduction [13].

Concerning the effect of polarization and regardless the cell, it is observed that the R_p value gradually decreases by increasing the polarization, implying improved charge transfer and electrode processes which occur at the HF arc [14]. In this respect, the most obvious differences between the cells, that caused the increase of polarization, are observed in the ohmic characteristics (R_s value). Specifically, for the cell with Ni/GDC the increase of the applied polarization resulted in the drastic deterioration (increase) of R_s. This trend can be attributed to the possible gradual re-oxidation and/or agglomeration of Ni, due to the high partial pressures of steam and CO_2 in the reaction mixture. Steam and CO_2 are produced electrochemically during the SOFC operation (Eq. 4 and 5) and Ni/GDC was the most active sample for H_2O (and CO_2) production (**Fig. 3**).

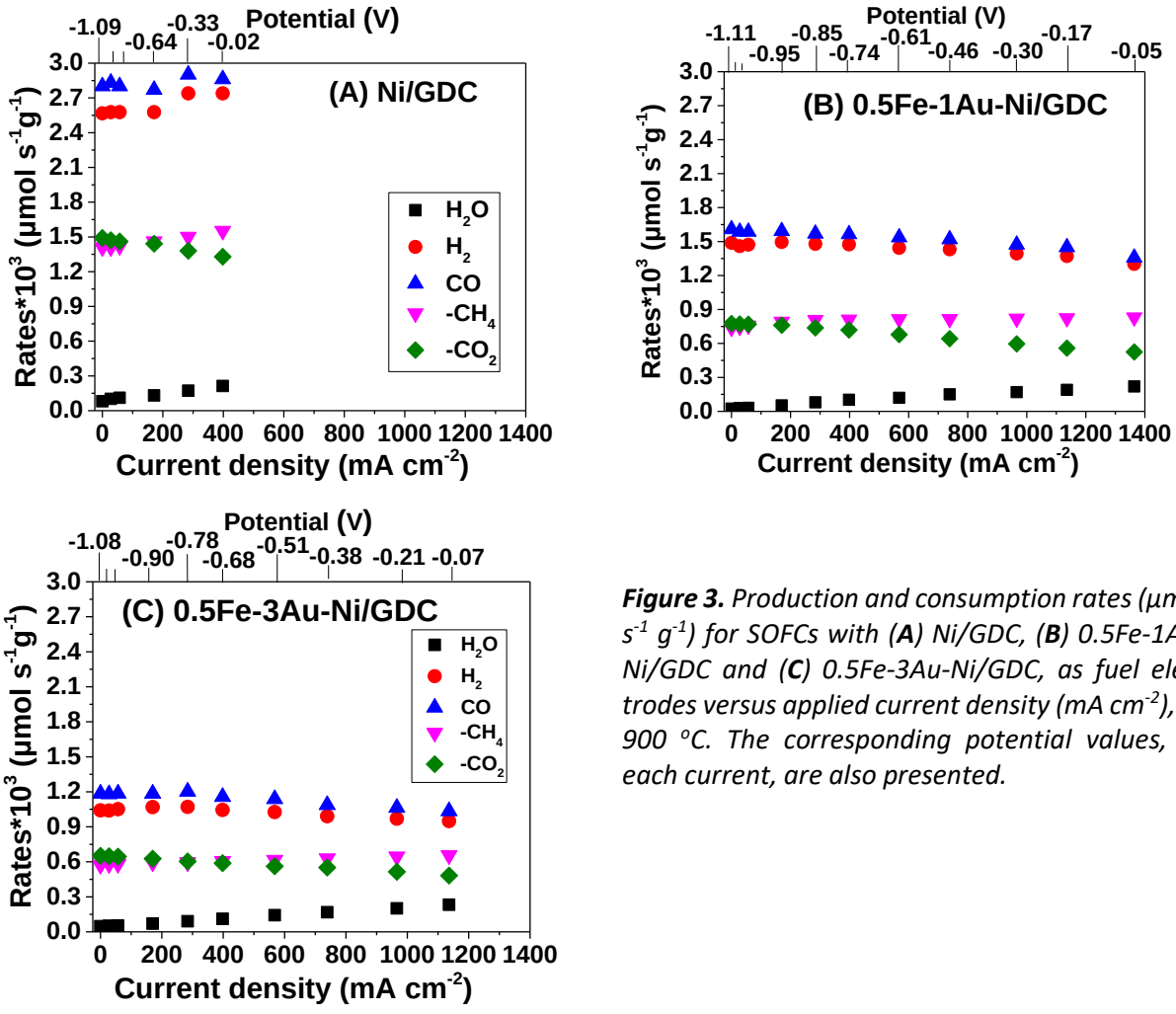

Figure 3. *Production and consumption rates (μmol s^{-1} g^{-1}) for SOFCs with (**A**) Ni/GDC, (**B**) 0.5Fe-1Au-Ni/GDC and (**C**) 0.5Fe-3Au-Ni/GDC, as fuel electrodes versus applied current density (mA cm^{-2}), at 900 °C. The corresponding potential values, at each current, are also presented.*

On the other hand, in the case of the cells with the modified electrodes the R_s value was the least deteriorated. More specifically, the R_s for the cell with 1Au-Ni/GDC was slightly increased, by increasing the applied polarization, while the R_s for the cell with 3Au-Ni/GDC remained practically the same. An interesting observation is the decreased R_s values for the cells with Fe and Au, under the highest polarization, indicating the improvement of their performances.

The outlet gas from the fuel side compartment was also analyzed under polarization conditions through GC measurements. **Fig. 3** exhibits the effect of the applied polarization for each cell on the consumption rates of CH_4, CO_2 and on the production rates of H_2, CO and H_2O. Regarding the effect of polarization on the production rates of H_2 and CO, it is observed that the increase of polarization causes increased r_{H2} and r_{CO} values for Ni/GDC, progressively decreased for 0.5Fe-3Au-Ni/GDC and 0.5Fe-1Au-Ni/GDC and fixed values for 3Au-Ni/GDC and 1Au-Ni/GDC (not shown here). High polarization resulted also in an increase in the production rate of H_2O for all samples. Nevertheless, the production of H_2O was not favored in the modified electrodes, compared to Ni/GDC, by applying the same current density values (i.e. up to 400 mA cm^{-2}). Although the modified electrodes achieved higher current densities than Ni/GDC under the same applied potential values, the latter exhibited overall higher rates. This can be attributed to the higher catalytic activity of Ni/GDC for the DRM reaction, as already detected in the half cell (catalytic) measurements of our previous work [13]. Despite the lower r_{H2} and r_{CO} of the modified cells, these values seem to be more than enough for the enhanced electrochemical operation, as also reported in the case of the internal CH_4 steam reforming reaction [12]. Furthermore, under fuel cell conditions carbon deposits were not detected, which may be correlated with the adsorbed carbon oxidation from O^{2-} species (Eq. 7).

ACKNOWLEDGMENTS

The research leading to these results has **received funding** from the European Union (co-funding) and Greek national funds through the operational program *'Regional Excellence'* and the operational program *'Competitiveness, Entrepreneurship and Innovation'*, under the call "**RESEARCH-CREATE-INNOVATE**" (Project code: **Eco-Bio-H2-FCs**, **Τ2ΕΔΚ-00955**) and from the **Fuel Cells and Hydrogen 2 Joint Undertaking (now Clean Hydrogen Partnership)** under the project **24_7 ZEN [Horizon Europe], Grant Agreement No 101101418**. This Joint Undertaking receives support from the European Union's Horizon 2020 Research and Innovation program, Hydrogen Europe and Hydrogen Europe Research. Views and opinions expressed are however those of the author(s) only and do not necessarily reflect those of the European Union or the Clean Hydrogen Partnership. Neither the European Union nor the granting authority can be held responsible for them.

REFERENCES

[1] Trendewicz AA and Braun RJ. (2013). *J. Power Sources*, 233, 380–393.
[2] Zhang H *et al.* (2021). *J. Power Sources*, 516, no. 230662.
[3] Saadabadi SA, Illathukandy B and Aravind PV. (2021). *Energy Sci. Eng.*, 9, no. 8, 1232–1248.
[4] Abdelkareem MA, Tanveer WH, Sayed ET, Assad MEH, Allagui A and Cha SW. (2019). *Renew. Sustain. Energy Rev.*, 101, 361–375.
[5] Yentekakis IV, Panagiotopoulou P and Artemakis G. (2021). *Appl. Catal. B Environ.*, 296, no. 120210.
[6] Escudero MJ, Maffiotte CA and Serrano JL. (2021). *J. Power Sources*, 481, no. 229048.
[7] Pakhare D and Spivey J. (2014). *Chem. Soc. Rev.*, 43, no. 22, 7813–7837.
[8] Souentie S, Athanasiou M, Niakolas DK, Katsaounis A, Neophytides SG and Vayenas CG. (2013). *J. Catal.*, 306, 116–128.
[9] Takahashi Y, Shiratori Y, Furuta S and Sasaki K. (2012). *Solid State Ionics*, 225, 113–117.
[10] Papadam T, Goula G and Yentekakis IV. (2012) *Int. J. Hydrogen Energy*, 37, no. 21, 16680–16685.
[11] Qiu P, *et al.* (2021). *Int. J. Hydrogen Energy*, 46, no. 49, 25208–25224.
[12] Neofytidis C, Dracopoulos V, Neophytides SG and Niakolas DK. (2018). *Catal. Today*, 310, 157–165.
[13] Ioannidou ET, Neophytides SG and Niakolas DK. (2024). *Energies*, 17, no. 1, 184.
[14] Zaravelis F and Niakolas DK. (2023). *Int. J. Hydrogen Energy*, 48, no. 94, 36663–36677.